Electrochemical Performances of Nanoparticle Fe 3 O 4 /Activated Carbon Supercapacitor Using KOH Electrolyte Solution

ARTICLE *in* THE JOURNAL OF PHYSICAL CHEMISTRY C · FEBRUARY 2009

Impact Factor: 4.77 · DOI: 10.1021/jp8088269

5 AUTHORS, INCLUDING:

Chengyang Wang
Technische Universität München
50 PUBLICATIONS **1,703** CITATIONS

SEE PROFILE

Ming-ming Chen
Tianjin University
61 PUBLICATIONS **1,783** CITATIONS

SEE PROFILE

Electrochemical Performances of Nanoparticle Fe_3O_4/Activated Carbon Supercapacitor Using KOH Electrolyte Solution

Xuan Du,[†] Chengyang Wang,*[,†] Mingming Chen,[†] Yang Jiao,[‡] and Jin Wang[†]

Key Laboratory for Green Chemical Technology of State Education Ministry, School of Chemical Engineering and Technology, Tianjin University, Tianjin 300072, People's Republic of China, and Northwest Electric Power Design Institute, Xi'an, Shaanxi 710032, People's Republic of China

Received: October 06, 2008; Revised Manuscript Received: December 14, 2008

In this study, activated carbon (AC)-Fe_3O_4 nanoparticles asymmetric supercapacitor cells have been assembled and characterized in 6 M KOH aqueous electrolyte for the first time. The nanostructure Fe_3O_4 was prepared by the microwave method. It only cost several minutes to prepare magnetite nanoparticles with average particle size of 35 nm. The electrochemical performances of the hybrid AC-Fe_3O_4 supercapacitor were tested by cyclic voltammetry, electrochemical impedance spectroscopy, and galvanostatic charge−discharge tests. The results show that the asymmetric supercapacitor has electrochemical capacitance performance within potential range 0−1.2 V. The supercapacitor delivered a specific capacitance of 37.9 F/g at a current density of 0.5 mA/cm^2. The result of cyclic characteristic test showed that it also can keep 82% of initial capacity over 500 cycles.

1. Introduction

Supercapacitors are considered one of the newest innovations in the field of electrical energy storage. They have many attractive characteristics such as low equivalent series resistance (ESR), long charge−discharge life, and high power density.[1,2] The growth in supercapacitors arose from displacing conventional battery and electrolytic capacitor products and from new market applications where existing technologies can not provide efficient solutions. According to the fundamental mechanisms that govern the capacitance, supercapacitors can be divided into two groups: (i) Electrical double layer capacitor (EDLC), where the capacitance attributed by the accumulation of charges at the electrode−electrolyte interface. The typical electrode material of EDLC is carbon materials with high surface area, such as activated carbon, carbon fiber, aerogel, etc.[3−5] (ii) Redox capacitors, where an actual battery-type oxidation−reduction reaction occurs leading to the pseudocapacitance. Metal oxides and conducting polymers belong to this kind of pseudocapacitance electrode materials.[6−8] In terms of long cycle-life and high specific capacitance, carbon has been recognized as promising electrode materials for EDLC. Because of the high specific capacitance (up to 250 F/g) of carbonaceous materials, they suffer from poor specific energy density[9] and limited cell voltage (limited to 1 V).[10] Recently, most research has focused on the hybrid supercapacitor because of their high working voltage and energy density. So far various metal oxides, such as RuO_2, CoO, IrO_2,[11−13] have been reported to be used as pseudocapacitance electrode materials. Applications of these materials have, however, been hindered by their high costs. Therefore, searching for less expensive pseudocapacitance material has been a major subject in supercapacitor research. Iron oxides are promising candidates because they are inexpensive and innocuous. Recently, the iron powder electrode was discovered that it showed capacitive characteristics from −1.4 to 1.0 V in alkaline solution.[14,15] In the works of Wu et al.,[16−18] they reported the capacitive characteristic of symmetric supercapacitor that used nanostructured Fe_3O_4 as the electrode material in mild aqueous electrolyte. According to their work, Fe_3O_4 nanocrystallites gave pseudocapacitance of 27 F/(g-Fe_3O_4) in mild aqueous electrolyte with an operation voltage range of 1.2 V. Moreover, Brousse et al.[19,20] studied the electrochemical performance of hybrid supercapacitor used Fe_3O_4 sub-micrometric particles and MnO_2 in mild aqueous electrolytes. The Fe_3O_4 not only complemented electrochemical window of MnO_2 but also showed promising application in hybrid supercapacitor. However, the main obstacle to overcome is the capacitance decrease caused by the poor cycling stability of MnO_2 in this hybrid system. So far, there is still no report on the hybrid supercapacitor fabricated with AC and Fe_3O_4 nanocrystallites to our best knowledge. In the present work, the electrochemical performances of AC-Fe_3O_4 hybrid supercapacitor using 6 M KOH electrolyte solution were investigated for the first time. Fe_3O_4 nanopaticles were obtained by microwave method, which is simple, convenient, and cheap compared with other methods.[16−18,21,22] The electrochemical performances of the hybrid supercapacitor were investigated by cyclic voltammetry (CV), electrochemical impedance spectroscopy (EIS), and galvanostatic charge/discharge tests.

2. Experimental Section

Fe_3O_4 powder was prepared by microwave method. Briefly, $FeSO_4 \cdot 7H_2O$ (Kewei Chemical Co. Ltd., Tianjin) was dissolved in distilled water, and then $NH_3 \cdot H_2O$ (Kewei Chemical Co. Ltd., Tianjin) was dropped into the solution. After being quickly stirred, the solution was heated in microwave oven (LG WD700; output power:700 W) for 8 min at 80 °C. The black precipitate was separated by magnet and washed repeatedly with distilled water. The resulting product was dried at 80 °C under moderate vacuum for 24 h. The resulted microstructural properties of prepared nanoparticle was characterized by nitrogen adsorption (Quantachrome NOVA 2000), X-ray diffraction (XRD; D/MAX 2500V/PC), and scanning electron microscopy (SEM; Philip

* To whom correspondence should be addressed. Phone: 86-022-27890481. Fax: 86-022-27890481. E-mail: cywang@tju.edu.cn.
[†] Tianjin University.
[‡] Northwest Electric Power Design Institute.

10.1021/jp8088269 CCC: $40.75
Published on Web 01/16/2009

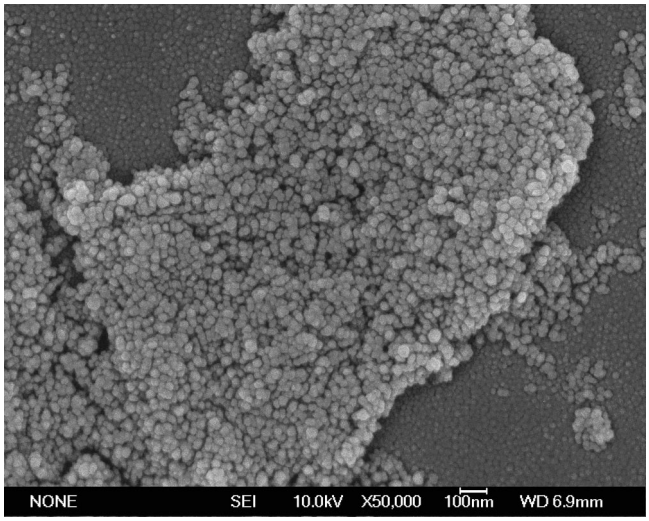

Figure 1. SEM image of Fe_3O_4 nanoparticles.

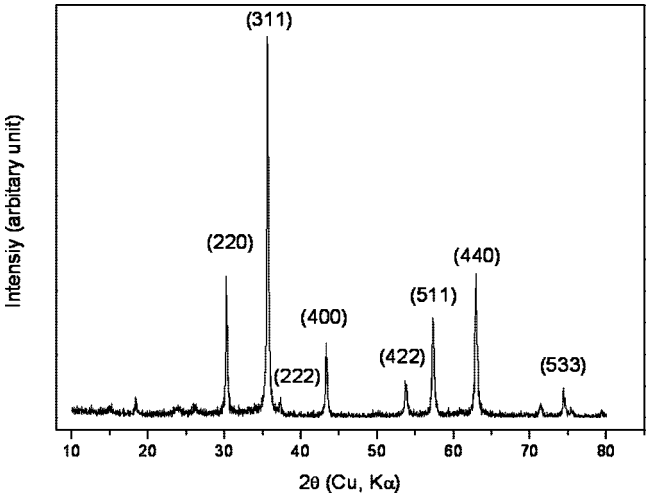

Figure 2. XRD of the Fe_3O_4 nanoparticles.

XL30). AC (Qingbao Co. Ltd., Beijing) with a specific surface area of 1197 m^2/g was used as received without further treatment.

The electrode of Fe_3O_4 nanoparticle was prepared according to the following steps. The mixture containing 80 wt % Fe_3O_4, 15 wt % acetylene black (AB), and 5 wt % polytetrafluoroethylene (PTFE) was well mixed and then was pressed onto a nickel grid (1.5×10^7 Pa) that serves as a current collector. The AC electrode was prepared by the same method as the negative electrode described above; it consisted of 85 wt % AC, 10 wt % AB, and 5 wt % PTFE. Then the Fe_3O_4 and AC electrodes were dried in a vacuum oven at 80 °C for 12 h to remove the solvent totally. The Fe_3O_4 composite electrode was separated from the AC composite electrode by a glass paper fiber wetted with the 6 M KOH solution. The three layers were then pressed in a coin-type cell (LIR 2430).

The CV and EIS measurements were performed on CHI 604A electrochemical analyzer (Shanghai, China) controlled by a computer. The CV experiments were carried out in a three electrode glass cell in 6 M KOH electrolyte. Platinum foil was used as a counter electrode and Hg/HgO as the reference electrode. The sweep rate of potential was set as 10 mV/s during CV testing. The EIS measurements were performed with a two-electrode cell. The Nyquist plots were recorded potentialstatically (0 V) by applying an AC voltage of 5 mV amplitude in the100 kHz−1 mHz frequency range. Galvanostatic charge/discharge cycle tests were performed on LAND Celltest (Wuhan, China). The charge and discharge current densities were ranged from 0.5 to 2 mA/cm^2 with cutoff voltage of 0−1.2 V for hybrid capacitor. The specific capacitance of the supercapacitor can be evaluated from the charge/discharge test together with the following equation

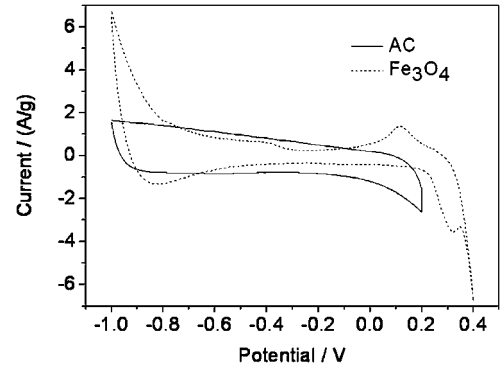

Figure 3. CV curves in a three-electrode cell using AC or Fe_3O_4 nanoparticles as working electrode, Pt as auxiliary electrode, and Hg/HgO as reference electrode in 6 M KOH solution. Scan rate of potential is 10 mV/s.

$$C_m = \frac{I\Delta t}{\Delta V m} \tag{1}$$

Where C_m is the specific capacitance of the capacitor (F/g), I is the current of the charge−discharge, and Δt is the discharging time period in seconds for the potential change ΔV, in volts. The m is the mass load of active materials (include positive and negative electrode). All electrochemical measurements were carried out at room temperature.

3. Results and Discussion

3.1. Characterization of Fe_3O_4. Figure 1 gives the SEM image of Fe_3O_4, which clearly indicates that the prepared material has aggregated particle consisting of average particle size of 30−40 nm. Figure 2 shows the X-ray diffraction pattern of magnetite, which is consistent with the results reported previously.[16] The reflections show that Fe_3O_4 powder contains magnetite as the predominant iron-containing species, except for a small amount of hematite. The crystalline size estimated according to Debye−Scherrer equation based on the line-broadening the magnetite (311) reflection is 34.5 nm. The surface area determined from Brunauer−Emmett−Teller measurements is 25 m^2/g, which can be translated into a grain size of 46 nm for nonagglomerated, nonporous crystallites according to the following equation

$$S = 6/(\rho D_m) \tag{2}$$

3.2. Electrochemical Studies. ***3.2.1. CV Test.*** CV was considered to be a suitable tool for estimating the difference between the non-Faradic and Faradic reactions. Figure 3 shows CV curves obtained in a three-electrode cell for the AC and Fe_3O_4 electrodes at voltage scan rate of 10 mV/s in 6 M KOH electrolyte using a Pt wire as auxiliary electrode and Hg/HgO as reference electrode. In Figure 3, it can be observed that the two materials are stable in a different range of potentials. The CV curve of AC has a rectangular shape within a potential window of −1 to 0 V (vs Hg/HgO), which is the character of double layer capacitance. However, when the potential increased to 0.2 V, the hydrogen evolution has become increasingly

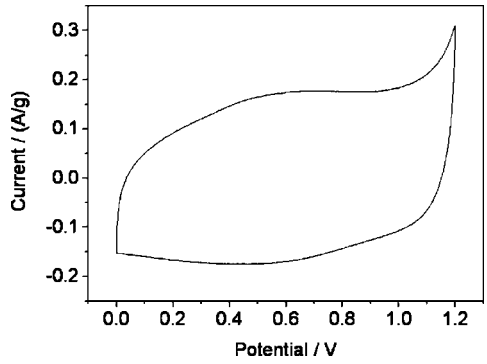

Figure 4. Cell CV curves for the hybrid Fe_3O_4 nanoparticles/AC supercapacitor at a scan rate of 5 mV/s in the voltage range from 0 to 1.2 V in 6 M KOH solution.

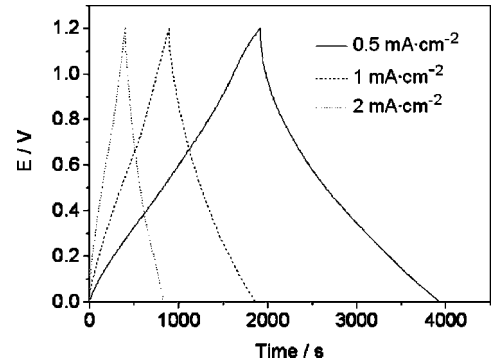

Figure 5. Charge/discharge curves of the hybrid Fe_3O_4 nanoparticles/AC supercapacitor at different current densities in 6 M KOH solution.

obvious. As for Fe_3O_4, two redox peaks at 0.1 and 0.3 V vs Hg/HgO were clearly observed. The anodic wave centered at about −0.3 V vs Hg/HgO that represents the active dissolution of the iron electrode which is associated with the generation of ferrate. The formation of ferrate during the anodic scan is confirmed by the observation of a cathodic wave which occurred between −0.2 and 0 V, which corresponds to the reduction of iron(VI) to iron(III).[14,15] The overall electrochemical behavior is in agreement with literature data and a complete description of the CV behavior in alkaline media, which is beyond the scope of this work, can be found elsewhere.[14,15,23,24] A more detailed study is required in order to clarify the influence of the magnetic on the potassium hydroxide redox reactions. By and large, the results in Figure 3 demonstrated that the Fe_3O_4 nanoparticles can be charge/discharged between −0.6 and 0.2 V vs Hg/HgO, and AC between 0 and −1 V versus Hg/HgO. The specific capacitance C (F/g) of a given electrode (AC or Fe_3O_4) was determined by integrating the cyclic voltammogram curve to obtain the voltammetric charge (Q), and subsequently dividing this charge by the mass of the composite electrode (m) and the width of the potential window (ΔE)

$$C = Q/(\Delta E m) \tag{3}$$

According to eq 3, the estimated specific capacitance of the Fe_3O_4 electrode is 58 F/g in the potential window −0.6 to 0.2 V vs Hg/HgO, and 90 F/g of AC electrode within the potential window −1 to 0 V. Subsequently, to ensure the charge balance of the hybrid cell, the weight ratio between the positive and negative electrodes was 1.5.

Figure 4 shows CV curves of the hybrid supercapacitor, which is fabricated with Fe_3O_4 positive electrode and AC negative electrode in 6 M KOH solution, at voltage scan rate of 5 mV/s in the potential range from 0 to 1.2 V. As shown in Figure 4, the rectangle shape of CV curve suggests that the asymmetric supercapacitor has electrochemical capacitance performance within the potential range (0−1.2 V).

3.2.2. Charge/Discharge Test. The applicability of supercapacitors can be directly evaluated by means of the galvanostatic charge−discharge method. Plot of voltage versus time for the AC-Fe_3O_4 supercapacitor at various current densities in KOH solution is given in Figure 5. As shown in Figure 5, a linear variation of the voltage was observed during the charging−discharging process, which can prove that the hybrid supercapacitor has good electrochemical capacitance performance.

On the basis of eq 1, the discharge specific capacitances of the hybrid capacitor at current densities were calculated. Figure 6 shows the dependence of specific capacitance on the discharge current density for the AC-Fe_3O_4 capacitor. The specific

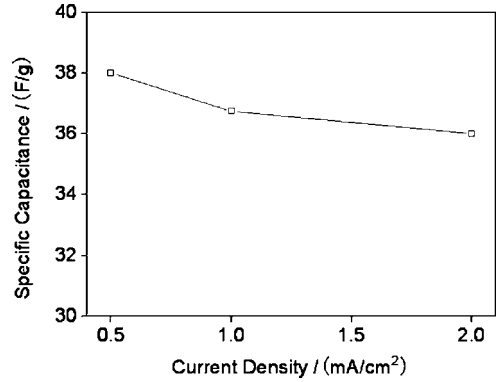

Figure 6. Dependence of the capacitance values of the hybrid supercapacitor on current density in a voltage range of 0−1.2 V.

capacitance of the AC-Fe_3O_4 capacitor is 37.9 F/g at a discharge current density of 0.5 mA/cm^2. In general, the specific capacitance decreases gradually with increasing discharge current density due to large IR drop at a large discharge current density that leads to the small specific capacitance. As could be expected, the specific capacitance of AC-Fe_3O_4 capacitor decreasing with the increasing of current density, which originates from the internal resistance of electrode. The specific capacitance of AC-Fe_3O_4 capacitor drops by 5.3% at high discharge current density of 2 mA/cm^2, which is caused by the IR drop of the resistive electrodes. According to the above results, the capacitance of supercapacitor is obviously higher than that of Fe_3O_4 symmetric capacitor reported in detail in literature,[16,17] in which the capacitance of Fe_3O_4 electrode is 27 F/(g-Fe_3O_4).

The cycle life of the hybrid capacitor was examined at a current density of 1 mA/cm^2. The specific capacitance of hybrid supercapacitor is shown in Figure 7 as a function of cycle number (cycled between 0 and 1.2 V). There is a small decrease of capacitance in the first 100 cycles, which is due to the consumption of electrolyte caused by the irreversible reaction between the electrodes and electrolyte,[25] and then it remains almost constant. The cycling performance that the hybrid supercapacitor can keep 82% of initial capacity over 500 cycles was observed. This indicates the high stability of Fe_3O_4 is suitable for high-performance hybrid supercapacitor applications.

3.2.3. EIS. The EIS measurements of both AC-AC symmetric capacitor and AC-Fe_3O_4 hybrid capacitor (at applied potential of 0 V; the frequency range is 10^5 to 10^{-3} Hz) were carried out, and a typical plot is shown in Figure 8. Three distinct regions are shown in Figure 8. In the low-frequency region, the impedance plots of both AC-AC symmetric capacitor and

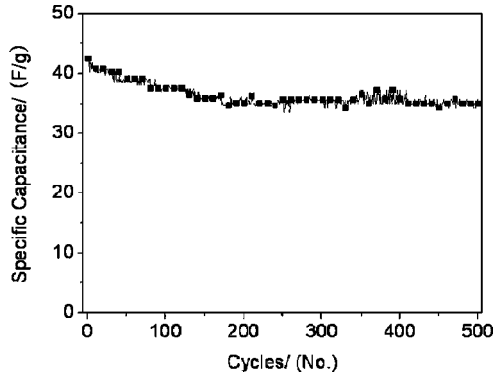

Figure 7. Variation of specific capacitance as a function of cycle number for AC-Fe_3O_4 supercapacitor.

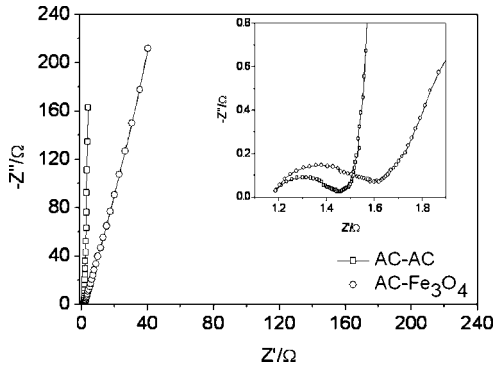

Figure 8. Nyquist plot of AC-AC and AC-Fe_3O_4 supercapacitors. (Inset: enlarged high-frequency region of Nyquist plot.)

AC-Fe_3O_4 hybrid capacitor increase and tent to become purely capacitive (vertical lines characteristic of a limiting diffusion process). In the intermediate frequency region is the 45° line that is the characteristic of ion diffusion into the electrode materials. In Figure 8, the semicircles, which represented the charge transfer resistance at the electrode/electrolyte interface, can be easily detected in the high frequency range of the plots. In addition, from their point intersecting with the real axis, the internal resistances (R_i) of these supercapacitors are about 1.2 Ω. As can be seen from the Nyquist plot, there were some differences between AC-AC and AC-Fe_3O_4 supercapacitors. The major difference was the AC-Fe_3O_4 capacitor showed a slight larger semicircle than AC-AC capacitor in the high frequency range, indicating a higher charge transfer resistance caused by oxidation of magnetite surfaces under the highly alkaline condition to form an insulating Fe_2O_3 layer, which can be indicated by the irreversible oxidation process noticed during the oxidative scan near the high-potential end.[18] Another difference was the straight line inclined at an angle of around 45° to the real axis (Z′) in the intermediate-frequency region, corresponding to the semi-infinite ion diffusion resistance. As shown in Figure 8, the differences between the Nyquist plots of the two supercapacitors reflected different energy storage mechanisms of AC and Fe_3O_4 electrodes.

4. Conclusions

In this study, it was only cost 8 min to prepare nanostructured Fe_3O_4 with an average particle size of 35 nm by the microwave method. In comparison with electrocoagulation and coprecipitation, this method is simpler, faste,r and cheaper. In addition, Fe_3O_4 nanoparticles were for the first time introduced to be positive electrode to fabricate a hybrid supercapacitor with activated carbon in 6 M KOH solution. The results of CV, EIS, and the charge/discharge measurements proved that this kind of hybrid supercapacitor has good electrochemical capacitance performance within potential range from 0 to 1.2 V. At a current density of 0.5 mA/cm^2, the hybrid supercapacitor delivered a specific capacitance of 37.9 F/g, which is much higher than that of Fe_3O_4 symmetric supercapacitor reported in literatures. The result of cyclic characteristic test showed that AC-Fe_3O_4 hybrid supercapacitor also can keep 82% of initial capacity over 500 cycles. In this respect, the AC-Fe_3O_4 hybrid supercapacitor is expected to extend the palette of available candidates in hybrid supercapacitor research, and a new path is open for future development of safe and cost-effective electrochemical supercapacitors.

Acknowledgment. Financial support from 863 Program of China (No. 2006AA11A161) and the Natural Science Foundation of Tianjin (No. 08JCZDJC17000) are acknowledged.

References and Notes

(1) Burke, A. *J. Power Sources* **2000**, *91*, 37.
(2) Conway, B. E. *Electrochemical Super capacitor and Technological Applications*; Kluwer-Plenum Press: New York, 1999.
(3) Yoshida, A.; Nonaka, S.; Aoki, I.; Nishino, A. *J. Power Sources* **1996**, *60*, 207.
(4) Nagawa, H.; Shudo, A.; Miura, K. *J. Electrochem. Soc.* **2000**, *147*, 38.
(5) Mayer, S. T.; Pekala, R. W.; Kaschmitter, J. L. *J. Electrochem. Soc.* **1993**, *140*, 446.
(6) Hu, C. C.; Huang, Y. H. *Electrochim. Acta* **2001**, *46*, 3431.
(7) Takasu, Y.; Murakami, Y. *Electrochim. Acta* **2000**, *45*, 4135.
(8) Li, W.; Chen, J.; Zhao, J.; Zhang, J.; Zhu, J. *Mater. Lett.* **2005**, *59*, 800.
(9) Qu, D.; Shi, H. *J. Power Sources* **1998**, *74*, 99.
(10) Cottineau, T.; Toupin, M.; Delahaye, T.; Brousse, T.; Belanger, D. *Appl. Phys. A: Mater.* **2006**, *82*, 599.
(11) Zheng, J. P.; Jow, T. R. *J. Electrochem. Soc.* **1995**, *142*, 6.
(12) Grupioni, A. A. F.; Lassali, T. A. F. *J. Electrochem. Soc.* **2001**, *148*, 1015.
(13) Skowronski, J. M.; Jurewicz, K. *J. Power Sources* **1993**, *45*, 263.
(14) Koninck, M. D.; Brousse, T.; Belanger, D. *Electrochim. Acta* **2003**, *48*, 1425.
(15) Denvir, A.; Pletcher, D. *J. Appl. Electrochem.* **1996**, *26*, 815.
(16) Wu, N. L.; Wang, W. Y.; Han, C. Y.; Wu, D. S.; Shiue, L. R. *J. Power Sources* **2003**, *113*, 173.
(17) Wang, S. Y.; Wu, N. L. *J. Appl. Electrochem.* **2003**, *33*, 345.
(18) Wang, S. Y.; Ho, K. C.; Kuo, S. L.; Wu, N. L. *J. Electrochem. Soc.* **2006**, *153*, 75.
(19) Brousse, T.; Belanger, D. *Electrochem. Solid State Lett.* **2003**, *6*, 244.
(20) Cottineau, T.; Toupin, M.; Delahaye, T.; Brousse, T.; Belanger, D. *Appl. Phys. A: Mater.* **2006**, *82*, 599.
(21) Cui, S.; Shen, X. D.; Lin, B. L. *Bull. Chin. Ceram. Soc.* **2006**, *25*, 48.
(22) Chen, A. H.; Wang, H. Q.; Zhao, B.; Li, X. Y. *Synth. Met.* **2003**, *139*, 411.
(23) Denvir, A.; Pletcher, D. *J. Appl. Electrochem.* **1996**, *26*, 823.
(24) Koninck, M. D.; Belanger, D. *Electrochim. Acta* **2003**, *48*, 1435.
(25) Wang, Y. G.; Xia, Y. Y. *J. Electrochem. Soc.* **2006**, *153*, 450.

JP8088269